Available online at www.sciencedirect.com

SCIENCE DIRECT®

Earth and Planetary Science Letters 233 (2005) 45–59

EPSL

www.elsevier.com/locate/epsl

Thermal and visual time-series at a seafloor gas hydrate deposit on the Gulf of Mexico slope

Ian R. MacDonald[a,*], Leslie C. Bender[b], Michael Vardaro[b], Bernie Bernard[c], James M. Brooks[c]

[a]*Texas A&M University-Corpus Christi, PALS, Corpus Christi, TX 78412, USA*
[b]*Texas A&M University, GERG, College Station, TX 77843, USA*
[c]*TDI-Brooks Int'l Inc, 1902 Pinion, College Station, TX 77845, USA*

Received 22 April 2004; received in revised form 31 January 2005; accepted 1 February 2005
Available online 29 March 2005
Editor: E. Boyle

Abstract

Ambient temperature is a critical factor determining the stability of gas hydrate deposits on continental margins. To study this process directly under varying conditions, a monitoring array comprising a time-lapse camera and in-situ temperature probes was deployed at a hydrocarbon seep known as Bush Hill, where gas hydrates deposits are exposed at the seafloor in a water depth of 570 m. For intervals of 91 days and 30 days, the digital camera recorded several daily images of a prominent gas hydrate mound consisting of structure II gas hydrate. The temperature probes were constructed with one autonomous thermistor at each end of a 50-cm PVC wand and recorded temperatures with precision of better than 0.1 °C at 30-min intervals over 327 days. One probe was implanted with a tight seal into a drill hole about 7 cm deep in the top of the gas hydrate mound. The second was inserted about 50 cm deep into the adjacent sediments. For each probe, the top thermistor recorded the ambient water temperature, while the bottom thermistor synoptically recorded the internal temperature of the hydrate or sediment. The bottom water temperatures ranged from 6.64 to 9.73 °C with a mean of 7.90 °C and standard deviation of 0.437. Photographic results showed no dramatic changes in the size, shape or gas venting from the mound. By comparing the temperatures recorded at the tips of the probes with the synoptic water temperature, we estimate that thermal diffusivity for the gas hydrate deposit was $7.14 \cdot 10^{-8}$ to $8.33 \cdot 10^{-8}$ m^2 s^{-1} and was $1.77 \cdot 10^{-7}$ to $3.01 \cdot 10^{-7}$ m^2 s^{-1} for the sediments at the sites where temperatures were recorded. The diffusivity measured in gas hydrate was lower than that measured under laboratory conditions. Stability of gas hydrate in this setting is not likely to be affected by short-term changes in bottom water temperature within the range observed.

Keywords: thermal diffusion; thermal conductivity; gas seep; bottom water temperature

* Corresponding author.
E-mail address: imacdonald@falcon.tamucc.edu (I.R. MacDonald).

0012-821X/$ - see front matter © 2005 Elsevier B.V. All rights reserved.
doi:10.1016/j.epsl.2005.02.002

1. Introduction

Ice-like deposits of gas hydrate in continental margin sediments comprise a very significant global reservoir of hydrocarbon [1]. Submarine gas hydrate forms and persists within a stability field defined by gas solubility, pressure and temperature [2]. Because climate cycles change sea level and bottom water temperature, ambient conditions for gas hydrate deposits vary and stability thresholds may be periodically exceeded over geologic time (e.g. [3,4]). The release of methane into ocean in the event of large scale decomposition of the gas hydrate reservoir has been proposed as the cause of excursions in $\Delta^{13}C$, which have been detected in benthic foraminifera from the late Paleocene [5] and glacial interstadials throughout the Quaternary [6]. The significance of this carbon for global warming or cooling is of intense interest and there have been numerous attempts to understand temperature and pressure controls upon hydrate formation and destabilization (e.g. [4,7,8]). However, most of the global gas hydrate reservoir occurs as strata buried beneath 100 to 300 m of sediment [9] and is detected because associated free gas produces a seismic anomaly known as a bottom-simulating reflector (BSR). In this setting, gas hydrate is well-insulated from most variations in pressure or temperature that occur during the present day and there is no possibility to observe directly the physical properties of naturally occurring gas hydrate in response to changing conditions.

Gas hydrate can also form at or near the seafloor where the flux of gas is rapid and prolonged. Seafloor deposits of gas hydrate were first reported from the Black Sea circa 1974 ([10], cited in [11]) and were collected in the northern Gulf of Mexico in piston cores circa 1983 [12]. Such deposits have subsequently been described from moderate depths (~500 to 1000 m) in diverse coastal margins including the Caspian Sea [13], the Okhotsk Sea [14], the northwestern United States [15,16], the western coast of Africa [17] and the southeastern United States [18].

Seafloor deposits often form distinctive mounds, ridges and faults [19], and manifest gas flux as streams of bubbles [20,21]. In this setting, gas hydrate deposits are subject to much more dynamic solubility, temperature and pressure regimes than are BSR deposits and thus provide a means to investigate the stability and thermal properties of gas hydrate under varying conditions. Previous studies have demonstrated significant increases in bubble flux over time scales of <24 h during intervals that corresponded to rising bottom water temperature [22,23]; these authors speculated that rising temperature caused the increased flux. Examples of cratering or local disturbances in the seafloor near gas hydrate deposits have also been noted [22,24]; these have been interpreted as possible evidence that pieces of gas hydrate spontaneously detached from the seafloor and floated upward in the water column—a process that could convey large quantities of gas into the mixed layer of the ocean or into the atmosphere. We conducted this study to measure directly the thermal diffusivity of natural, structure II gas hydrate and to how examine hydrate mound morphology is altered on a yearly time-scale.

2. Study site

In the Gulf of Mexico, rapid flux of thermogenic gas has produced numerous settings where gas hydrate occurs as lens-like deposits that are partially exposed to water or buried beneath a few centimeters of sediment [8]. The experiments described in this paper were carried out at Bush Hill, which is a well-known hydrocarbon seep and gas hydrate deposit located at 570 m depths southwest from the Mississippi Delta (Fig. 1A) at the top of a ~500 m wide, ~40 m high topographic high [19]. Persistent mounds of gas hydrate are found near the top of the feature (Fig. 1B). Bubbles of gas and drops of oil vent continually from fissures in the gas hydrate deposit and orifices concealed by sediment or mussel beds [21]. Previous studies [25] showed that the temperature regime at Bush Hill was dynamic; these authors reported mean temperatures of 7.9 °C (S.D. 0.49) in 1993–1994, 8.0 °C (S.D. 0.58) in 1994–1995 and 7.5 °C (S.D. 0.50) in 1997–1998. Detailed photographic records indicate that the morphology of gas hydrate deposits can alter significantly from year to year [19,22]. The source gases at Bush Hill include ethane, propane, butane and traces of pentane; consequently, gas hydrate occurs as a structure II crystal and includes significant traces of crude oil as well as sediment and organic material [26]. At this depth, the stability temperature for structure II gas hydrate is

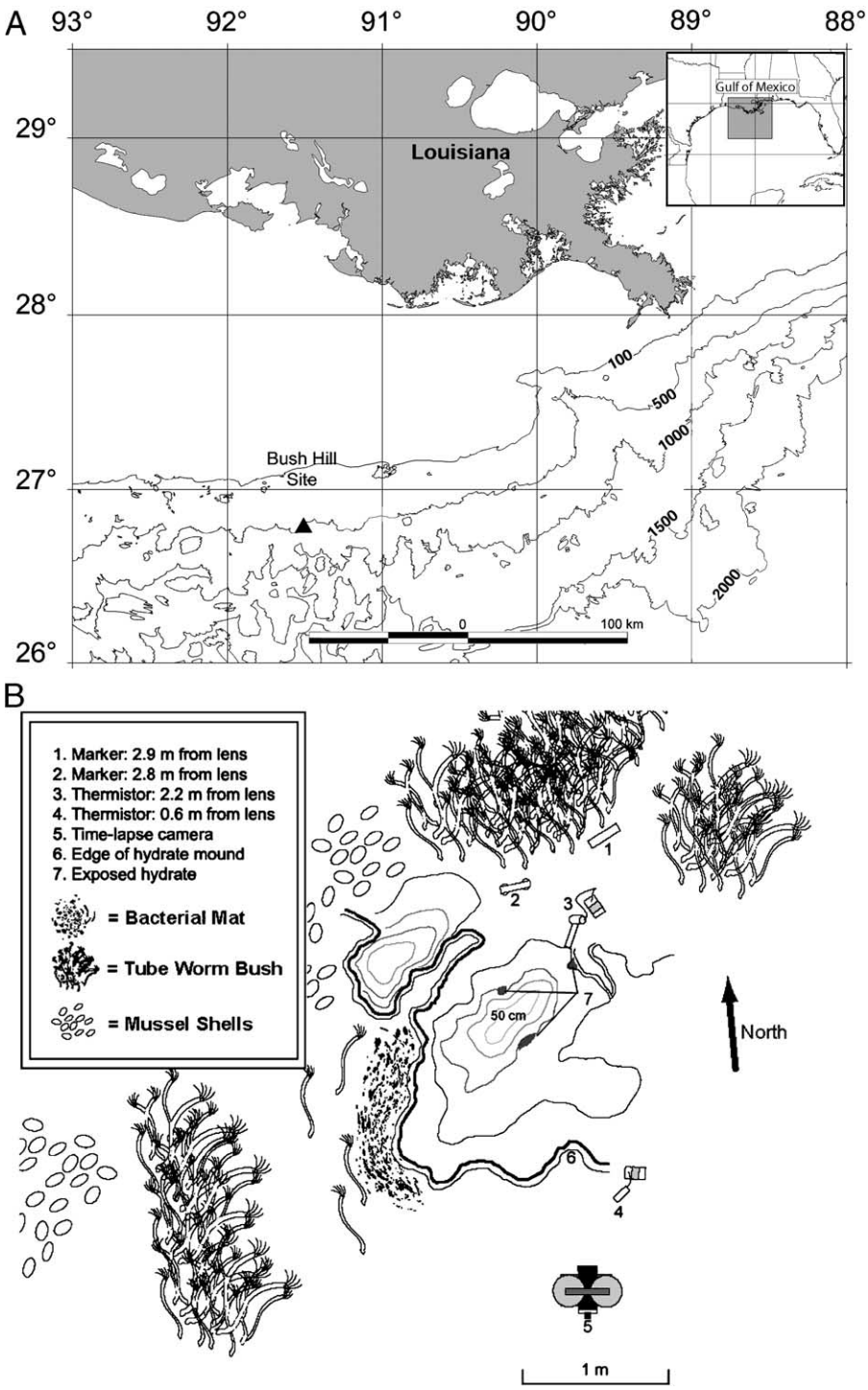

Fig. 1. Map of Bush Hill shows the location of study site in Gulf of Mexico region (A). Detail of gas hydrate deposit shows how thermistor probes and time-lapse camera were situated for experiment (B). Relief of gas hydrate mound indicated by contours, which are approximately 10 cm.

about 16 °C [27]. The deposits are biologically significant as substrata for microbial and metazoan colonization, which may have direct or indirect effects on persistence of gas hydrate deposits and the sediment overlying them [19,28,29].

3. Materials and methods

Simple thermal probes were constructed from Antares® recording thermistors secured in 2-cm PVC pipe. The PVC probes were 50 cm long and fabricated so that one thermistor tip was exposed at each end (Fig. 2A). The thermistors were programmed to record temperatures at 30-min intervals with a precision of 0.01 °C. Working with the Johnson Sea Link Submersible and a specially designed drill, we bored 2 cm diameter holes 7 to 9 cm deep into the top of a prominent gas hydrate mound at Bush Hill (Fig. 2B). Drill cores of gas hydrate (Fig. 2C) recovered in an insulated pressure vessel confirmed that the gas hydrate deposit was a solid mass of clathrate. The

Fig. 2. Photographs of equipment and samples used in the observations: thermistor probes were fabricated from PVC pipe and Antares® recording thermistors (A); a hydraulic drill was used to bore holes into the gas hydrate deposit (B); recovered gas hydrate contained oil and sediment inclusions (C); a time-lapse camera was used to monitor the morphology of the hydrate deposit and the integrity of the thermistor implants.

PVC probes were then inserted into these holes with a tight seal. Alternately PVC probes were inserted 50 cm deep into the sediment immediately adjacent to the mound. Thus, the probes could record water temperatures from the top thermistors on both probes and internal temperatures within the hydrate and the adjacent sediments at depths of 7–9 cm and 50 cm, respectively. Thermistors were inter-calibrated pre- and post-deployment by bundling groups of them together and carrying them to the bottom in a semi-enclosed bucket on the submarine, while recording temperatures at 0.5-s intervals. This procedure measures temperatures over an appropriate range within a uniform temperature field.

To verify the continued integrity of the thermistor probes, and to monitor the daily changes in the hydrate mound and its biological community, a digital camera (Fig. 2D) was emplaced about 1 m away from the edge of the mound and about 2 m away from the thermistor probes (Fig. 1B). The camera, a modified Nikon Coolpix® 990, was configured to take a picture every 6 h. Illumination was provided by a pair of 50-W quartz lamps, which were powered by a 12-V gel cell battery. Probes and camera were deployed on 18 July 2001 and recovered on 6 June 2002. The camera and a second set of probes were briefly redeployed on 3 June and recovered for the final time on 3 July. The camera was repositioned very close to its original vantage point during June 2002, so the time-study of the deposit could be continued. During the second camera deployment, photographs were taken every 2 h.

4. Results

Battery power to the camera and lamps lasted for 91 days during the long-term deployment and resulted in 373 images showing the gas hydrate mound, the thermistor probes, the sediment cover and patches of exposed hydrate, as well as the mobile fauna and bacterial mats that inhabited the mound area (Fig. 3A–B). The second deployment resulted in 361 images showing essentially the same vantage of the mound as the previous series (Fig. 3C–D). This record showed that the morphology of the deposit was little altered over a total observation period of 350 days, although comparison between 2001 and 2002 indicate and slight overall increase in size. It remained a low

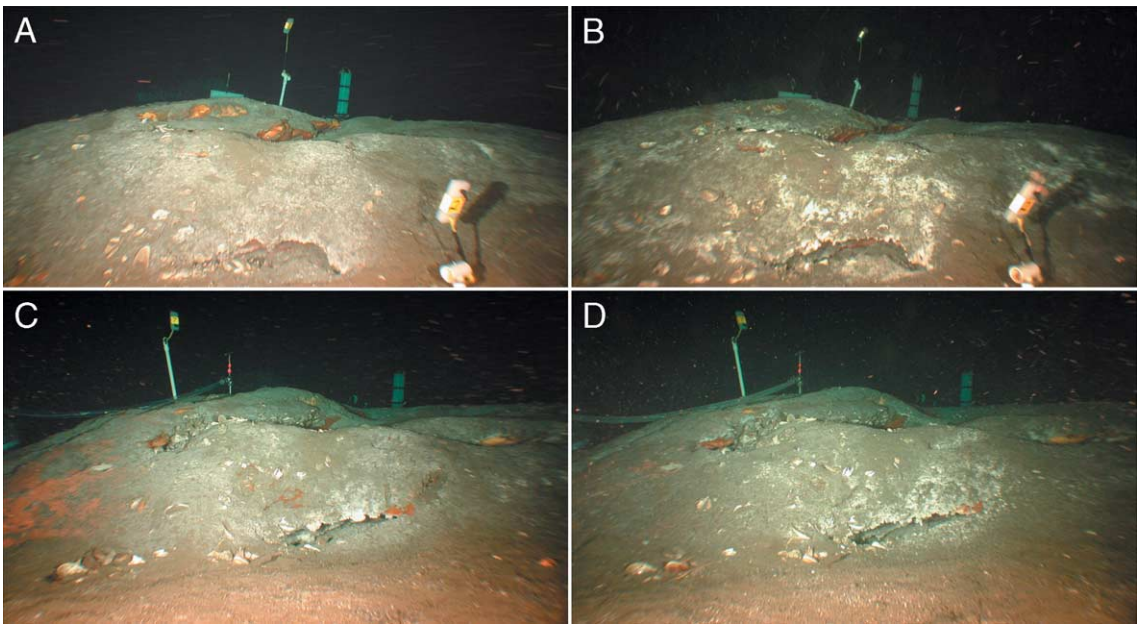

Fig. 3. Digital photographs of the hydrate mound were collected over a total interval of 350 days. The first interval comprised day 0 to day 91 (A–B). The second interval comprised day 329 to day 350 (C–D).

mound, approximately 2.5 m wide and about 0.65 m high. The sediment cover was continually colonized by bacterial mats, but the extent of these mats varied from day to day due to disturbances by crabs, sea stars and molluscs. The most pronounced changes were crevices of exposed hydrate on the down-slope margin of the mound. These crevices harbored diverse biological activity including fishes, molluscs and annelid worms. Importantly, the visual record confirmed that the thermistor probes remained in place as they were inserted and undisturbed during the experiments.

The long-term thermistor deployment yielded a 327-day record of water temperature and the internal temperature of gas hydrate and sediment at probe depths of 7 cm and 50 cm, respectively (Fig. 4A). Considering the water temperature first, this record shows that bottom water temperature had a mean of 7.90 °C (standard deviation of 0.437) and exhibited repeated excursions within a range of about 3 °C. Greatest range in temperature fluctuation in bottom water occurred during March 2002 when temperature increased from 6.64 °C to 9.73 °C in 20 days. We expand the scale for this interval to illustrate the characteristics of variation (Fig. 4B). In the expanded record, a higher frequency of variation becomes evident in the bottom water temperatures. The low frequency fluctuations over a range of about 3 °C are overprinted with a more rapid oscillation of about 0.25 to 0.5 °C. Comparison of water temperature with synoptic temperatures internal to the gas hydrate deposit or adjacent sediment reveals that these substrata reflect similar trends of increase or decrease in temperature, but that the gas hydrate and sediment temperatures lag the water temperature by about 0.5 and 3 days, respectively. Moreover, the ranges of variability for the gas hydrate and sediment temperatures are notably reduced. The high-frequency oscillation is evident, but suppressed in the gas hydrate temperature record; it cannot be detected in the sediment temperature record.

Periodograms (FFT) of the complete, 327-day temperature records illustrate the periodic and episodic fluctuations of the temperature records. In the periodogram of the bottom water record, the strongest signal is at the K1 tidal frequency (23.9 h) with significant peaks at M2 (12.4 h) and 6 h (Fig. 5A). Possibly, these high frequencies are riding a longer-term, larger-scale variation that may be Rossby waves or eddy processes that take tens of days to develop. The K1 signal was present in the internal gas hydrate temperatures, while the higher frequency peaks were indistinct or absent (Fig. 5B). High frequency signals were completely suppressed in the internal temperatures of the sediments adjacent to the gas hydrate deposit (Fig. 5C).

It was apparent that the internal temperatures of gas hydrate and surface sediments are determined by heat flow from the bottom waters. The results were hydrate and sediment temperatures that tracked the trend of water temperature with respectively greater damping of the high-frequency fluctuation and longer lags between the peaks. Notably, careful examination of the record does not show any evident separation of the hydrate and sediment temperatures from the bottom water cycles and trends. We therefore infer that the geothermal gradient has been constant during our record and that heat flow has not been perturbed by episodic gas or fluid venting. Analysis of the records can therefore provide estimates for the thermal diffusivity of hydrate and sediments. The analytical approach is outlined below.

In a homogeneous semi-infinite, half space the temperature T at depth z due to a time-varying surface temperature change is governed by the one-dimensional heat diffusion equation with the appropriate boundary and initial conditions [30]:

$$\frac{\partial T}{\partial t} = \alpha \frac{\partial^2 T}{\partial z^2} \tag{1}$$

where t is the time and α is the thermal diffusivity with units of length^2 time^{-1}. Here we assume that there is no advection of heat by fluid flow, which is assured when the probe fits snugly in the drilled hole. This equation represents a different process that is occurring in the field than what is typically measured in the laboratory using the von Herzen and Maxwell needle probe method. As a consequence, the thermal diffusivity is measured in the field, not the thermal conductivity.

Eq. (1) is best solved numerically. The simplest approach discretizes (1) across a very coarse grid, that of the spacing between the surface and the probe:

$$\frac{T_{\mathrm{p}}^{n+1} - T_{\mathrm{p}}^{n}}{\Delta t} = \alpha \frac{T_{\mathrm{w}}^{n} - 2T_{\mathrm{p}}^{n} + T_{\mathrm{geo}}^{n}}{\Delta z^2} \tag{2}$$

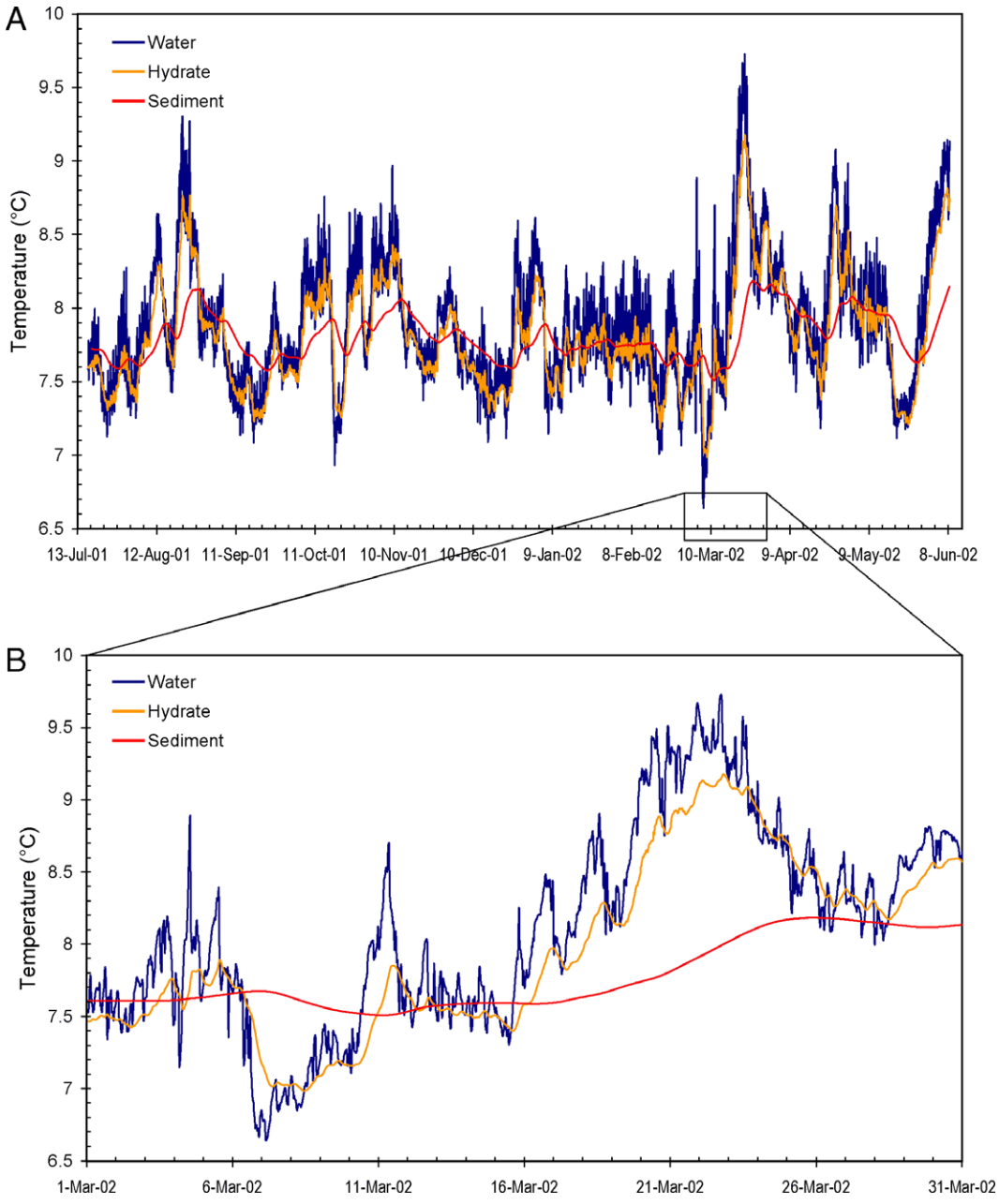

Fig. 4. The thermistor probe time-series show repeated episodes of bottom water temperature fluctuation during 327 days (A). Detail of the largest temperature swing shows that a high frequency variation was embedded in the month-long episode (B). Internal temperatures of gas hydrate and sediments track respond to the changing water temperatures after characteristic time lag.

In Eq. (2), we have represented the spatial derivative in (1) using a three-point centered difference approximation and the time derivative with a two-point forward difference approximation. The subscript on T represents the location on the z axis, where T_w represents the water temperature measured at the surface, T_p is the probe temperature and Δz is the measured probe depth. The temperature at T_{geo} is

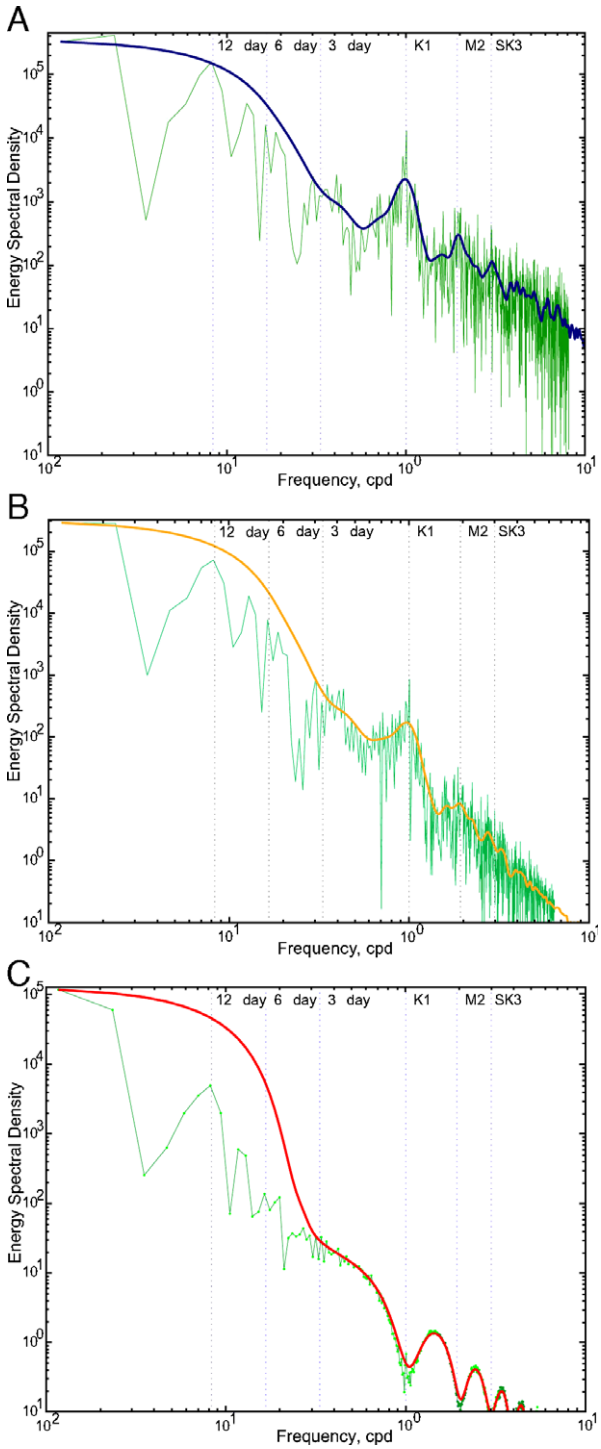

Fig. 5. FFT periodograms of the 327-day records for bottom water (A), gas hydrate (B) show distinct peaks at the K1 tidal frequency while this signal is lost in the records from the sediment probe (C).

an unknown that is determined by assuming a flux condition. The superscript represents the time step so that n+1 is Δt greater than n. Eq. (2) is typically referred to as the FTCS (forward in time centered in space) scheme. Rearranging (2) gives the following simple algorithm,

$$T_{\mathrm{p}}^{n+1} = T_{\mathrm{p}}^{n} + s\left(T_{\mathrm{w}}^{n} - 2T_{\mathrm{p}}^{n} + T_{\mathrm{geo}}^{n}\right) \tag{3}$$

where s is the modulus.

$$s = \alpha\frac{\Delta t}{\Delta z^2} \tag{4}$$

The temperature T_{geo} is an unknown that can be estimated by assuming that below the probe the heat flux is determined entirely by the geothermal flux,

$$q_{\mathrm{geo}} = k\frac{\partial T}{\partial z} \tag{5}$$

where k is the thermal conductivity of the hydrate given by

$$k = \alpha\rho C_{\mathrm{p}} \tag{6}$$

A two-point centered difference approximation of (5) yields

$$q_{\mathrm{geo}} = k\frac{T_{\mathrm{p}}^{n} - T_{\mathrm{geo}}^{n}}{\Delta z} \tag{7}$$

Solving for T_{geo} yields

$$T_{\mathrm{geo}}^{n} = T_{\mathrm{p}}^{n} - q_{\mathrm{geo}}\frac{\Delta z}{k} \tag{8}$$

Substituting (7) into (3) yields a simple linear relationship,

$$T_{\mathrm{p}}^{n+1} = T_{\mathrm{p}}^{n} + s\left(T_{\mathrm{w}}^{n} - T_{\mathrm{p}}^{n}\right) + b \tag{9}$$

where

$$b = -\frac{\Delta t}{\Delta z}\frac{q_{\mathrm{geo}}}{\rho C_{\mathrm{p}}}. \tag{10}$$

This is a straight-forward linear equation with two unknowns, s and b. The parameter b contains a combination of the geothermal flux and the density and heat capacity of the hydrate, but it does not need to be defined a priori. Given the time series of thermistor temperatures, the parameters s and b can be estimated with a least squares analysis. In this way, the thermistor experiment becomes an autoregressive problem in one-dimensional heat conduction.

An alternate and certainly more rigorous method of estimating the thermal diffusivity begins with a better finite difference approximation of (1) based on a fine scale grid and the application of the geothermal flux condition deep within the hydrate. We used a fully implicit method, the Crank-Nicholson scheme, for numerically solving (1) on a fine scale grid.

$$\frac{T_j^{n+1} - T_j^{n}}{\Delta t} = \alpha\left(\frac{1}{2}L_{xx}T_j^{n} + \frac{1}{2}L_{xx}T_{j+1}^{n}\right) \tag{11}$$

where $L_{xx}T_j = \frac{T_{j-1}-2T_j+T_{j+1}}{\Delta z^2}$. This scheme is unconditionally stable for any value of time and distance, but values were used that provided the best accuracy weighed against reasonable computational times. Eq. (11) expands to

$$T_j^{n+1} - T_j^{n} - s\left[\left(T_{j-1}^{n} - 2T_j^{n} + T_{j+1}^{n}\right) + \left(T_{j-1}^{n+1} - 2T_j^{n+1} + T_{j+1}^{n+1}\right)\right] = 0 \tag{12}$$

where $s = \frac{1}{2}\frac{\alpha\Delta t}{\Delta z^2}$. This leads to a tridiagonal system of linear equations

$$-sT_{j-1}^{n+1} + (1+2s)T_j^{n+1} - sT_{j+1}^{n+1} = d_j \tag{13}$$

where $d_j = sT_{j-1}^{n} + (1-2s)T_j^{n} + sT_{j+1}^{n}$

Given an initial condition for the temperature distribution and two boundary conditions, this equation can be readily solved for the next temperature distribution.

The boundary condition at the surface is simply that of the surface temperature record, which forces the response. The bottom boundary condition is that of geothermal flux, given by (5), but applied well below the surface at the depth of 100 cm. Increasing it to 200 cm makes a very minor change in the results. We assumed a value of 30 mW m^{-2} for the geothermal flux and a thermal conductivity of 0.49 W m^{-1} K^{-1} [31,32]. We note that the final value for the thermal diffusivity was particularly insensitive to these values. Finally, this model was tested against a known analytical solution in order to verify its accuracy.

Fig. 6A and B, respectively, show predicted internal temperatures of gas hydrate and sediment observed during the March 2002 episode temperatures

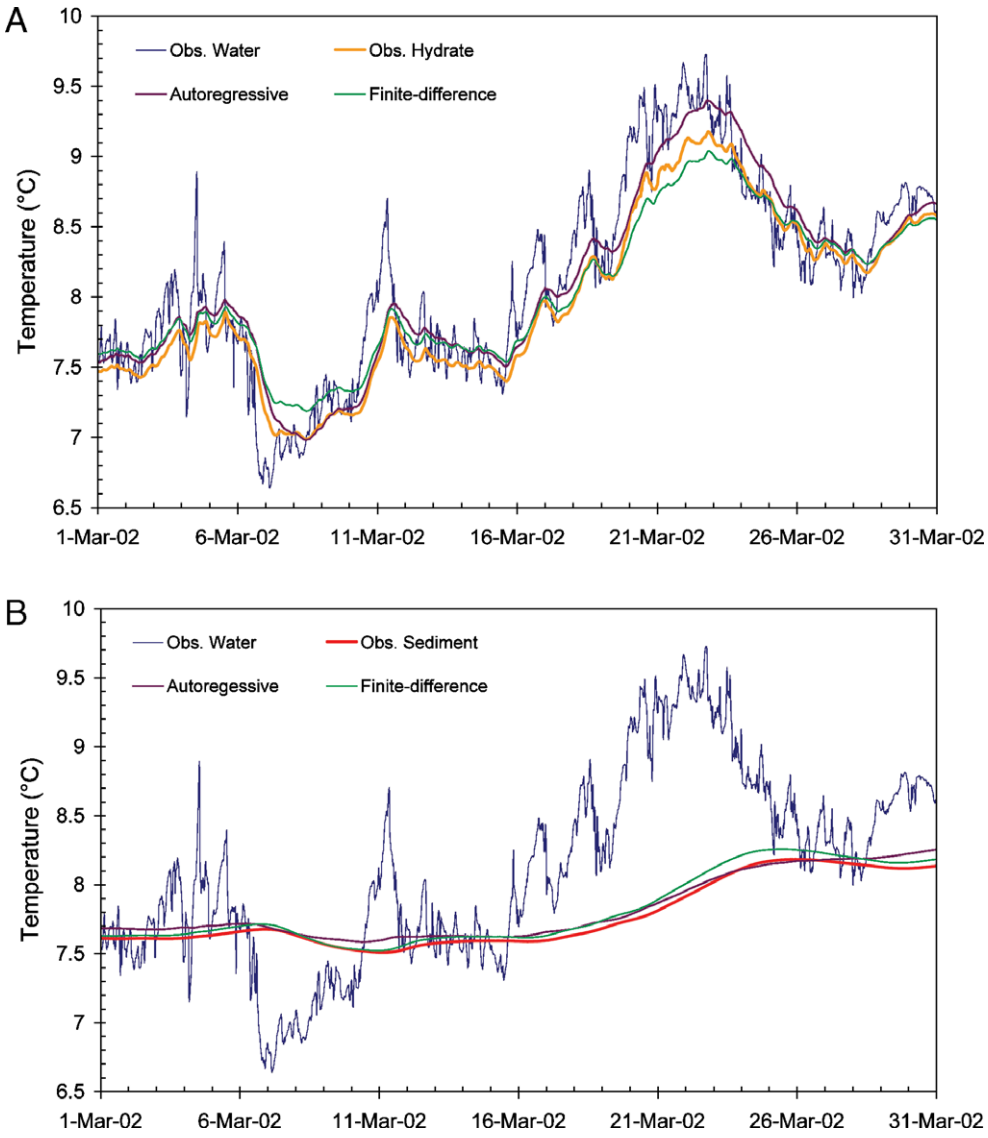

Fig. 6. Observed and predicted temperatures are plotted for gas hydrate (A) and sediment (B) during the major temperature swing. For details of fit, see Table 1.

predicted by estimating thermal diffusivity in hydrate and sediment. Results from autoregressive and finite-difference estimates are shown for comparison. The calculated values for thermal diffusivity in sediment and gas hydrate are shown in Table 1 along with values for ice and methane hydrate. The methane hydrate value was calculated from the density, conductivity and heat capacity reported in the literature. Davidson [31] reports a density of 0.912 g cm^{-3}, a constant pressure heat capacity of 0.576 mW h g^{-1} K^{-1} at 270 K and a thermal conductivity of 0.49 W/m K [31,32] for structure I methane hydrate ($CH_4 \cdot 6H_2O$) measured in the laboratory.

The fit of autoregressive and finite difference models was robust overall, but was challenged when water temperature exhibited prolonged increase or decrease, as was the case during March 2002. The differences between model-predicted temperatures

Table 1
Estimates of thermal diffusivity obtained from fitting autoregressive and finite element models to temperature records obtained from thermistor probes implanted into gas hydrate deposits and sediment adjacent to gas hydrate mound

Substratum	Length (cm)	Time (days)	Model	Thermal diffusivity ($m^2\ s^{-1}$)	R^2
Hydrate	7	327	Autoregressive	$7.14 \cdot 10^{-8}$	0.99
Hydrate	7	327	Finite difference	$8.33 \cdot 10^{-8}$	0.99
Hydrate	8	31	Autoregressive	$1.47 \cdot 10^{-7}$	0.99
Sediment	50	327	Autoregressive	$1.77 \cdot 10^{-7}$	0.91
Sediment	50	327	Finite difference	$3.01 \cdot 10^{-7}$	0.96
Sediment	16	31	Autoregressive	$2.12 \cdot 10^{-7}$	0.97
Water ice	–	–	Literature	$1.27 \cdot 10^{-8}$	–
Methane hydrate	–	–	Literature	$2.59 \cdot 10^{-7}$	–

Length indicates the depth of implantation.

and measured temperatures are summarized in Table 2.

As far as we are able to determine, there are no reported values of methane hydrate thermal diffusivity, or thermal conductivity, measured in the field. The field measured value of the thermal diffusivity of hydrate is $8.33 \cdot 10^{-8}$ $m^2\ h^{-1}$, which corresponds to a thermal conductivity of 0.135 W m^{-1} K^{-1}. Our reported value is three times lower than the 'standard' literature value. There are a number of possible explanations. The lack of a third thermistor deeper in the hydrate forces us to impose a boundary condition that may introduce additional errors. In addition, if there was fluid flow past the probe, then this would lower the measured thermal conductivity and it also might explain the high frequency response seen in the thermistor records.

Waite et al. [33] report a thermal conductivity of 0.347 W/m K for pure methane hydrate. This is significantly lower than the 'standard' value of 0.49 W/m K [27,32,33]. The difference in the values may be attributed to differences in the experimental design. Stoll and Bryan [34] were interested in the same problem as Waite. They modified the basic experimental procedure of von Herzen and Maxwell [35] to eliminate the possibility that the hydrate contained such a large volume of trapped gas that the overall conductivity of the mixture was lowered. Stoll and Bryan [35] accomplished this by including a stirring-compacting piston that could be simultaneously rotated and translated throughout the full length of the chamber. The end result was a compacted mixture that could contain no trapped gas. Waite et al. [33] cite this work, but only in the context that the mixture of sediment and pure methane hydrate is no longer well characterized. They go on to state that, despite past extensive laboratory work by several investigators, there is a lack of thermal conductivity data for well-characterized mixtures of sediment and pure methane hydrate. Consequently, Waite et al. do not disturb their mixture once it forms. Therefore, one could argue they get 'in situ-like' values, which may in fact contain trapped gas. Gas-filled porosity might explain their lower conductivity values, as well as our lower thermal conductivity.

Table 2
Mean differences between gas hydrate and sediment temperatures measured with implanted probes and predicted with autoregressive and finite difference models

Model (interval)	Predicted-measured T °C (% range)	
	Gas hydrate	Sediment
Autoregressive (327 days)	0.000 (0.01%)	0.002 (0.28%)
Autoregressive (31 days)	0.042 (0.57%)	−0.029 (4.99%)
Finite difference (327 days)	−0.002 (0.10%)	0.015 (2.25%)
Finite difference (31 days)	−0.018 (0.08%)	0.044 (6.47%)

Means were calculated for the entire 327-day interval shown in Fig 4A and for the 31-day interval shown in Figs. 4B and 6.

The effect of impurities contained within the hydrate can be estimated with a simple mixing concept, similar to that proposed by von Herzen and Maxwell [35]. The density of the mixture may be written as

$$\frac{1}{\rho_{\mathrm{mix}}} = w\left(\frac{1}{\rho_{\mathrm{impurity}}} - \frac{1}{\rho_{\mathrm{hydrate}}}\right) + \frac{1}{\rho_{\mathrm{hydrate}}}$$

where w is the weight fraction of the impurity in the hydrate, ρ_{impurity} is the density of the impurity and

Table 3
Properties of methane hydrate and various impurities

	Property		
	ρ (gm cm^{-3})	K (W m^{-1} K^{-1})	C (W h g^{-1} K^{-1})
Methane hydrate	0.912	0.49	$5.76 \cdot 10^{-4}$
Seawater	1.03	0.60	$10.9 \cdot 10^{-4}$
Ice	0.91	2.21	$5.35 \cdot 10^{-4}$
Quartz sand	1.52	0.35	$2.32 \cdot 10^{-4}$
Light oil	0.91	0.133	$5.00 \cdot 10^{-4}$

ρ_{hydrate} is the density of the hydrate. Similarly, the heat capacity is given by

$$C_{\text{mix}} = wC_{\text{impurity}} + (1-w)C_{\text{hydrate}}$$

where C_{impurity} is the constant pressure heat capacity of the impurity and C_{hydrate} is the constant pressure heat capacity of the hydrate. The heat conductivity is given by

$$K_{\text{mix}} = wK_{\text{impurity}} + (1-w)K_{\text{hydrate}}$$

where K_{impurity} is the thermal conductivity of the impurity and K_{hydrate} is the thermal conductivity of the hydrate. Finally, the diffusivity of the mixture is simply

$$\alpha_{\text{mix}} = \frac{K_{\text{mix}}}{\rho_{\text{mix}} C_{\text{mix}}}.$$

Using the physical properties of the various impurities [30] listed in Table 3, the estimated thermal diffusivity of the contaminated hydrate as a function of the weight fraction of the impurity is calculated and shown in Fig. 7A–D. These calcu-

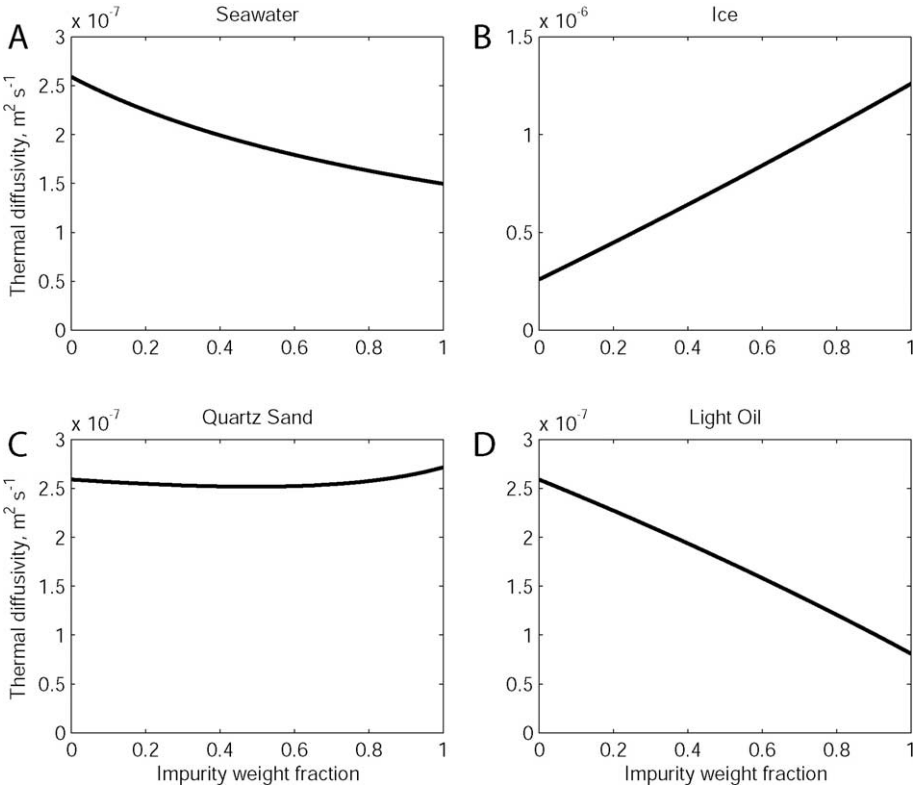

Fig. 7. The estimated change in the thermal diffusivity of pure methane hydrate as a function of increasing weight fraction for possible impurities: seawater (A), ice (B), quartz sand (C) and light oil (D).

lations indicate that seawater and/or oil within the gas hydrate would have the potential to lower the measured thermal diffusivity.

5. Discussion

These findings show that shallow deposits of gas hydrate on the continental slope in the Gulf of Mexico are subject to a dynamic and variable thermal regime, with a temperature range of 3 °C and excursions to 1.8 °C greater than the mean of 7.9 °C. Although time-series of comparable length have not been reported from gas hydrate deposits elsewhere, available information indicates that other localities where shallow hydrate deposits are found at slope depths exhibit lower mean temperatures at comparable depths and probably less variation over time. For example, Peltzer and Brewer [2] describe observations at the Eel River gas hydrate site offshore northern California and report ambient temperatures of ~6 °C at 515 m. These authors note that this was 0.4 to 0.5 °C warmer than when gas hydrates were collected at the site in 1991 [15]. Elsewhere, Hutnak et al. [36] report a 0.2° variation over 7 days at Hydrate Ridge offshore Oregon. Peltzer and Brewer [2] point out that any destabilization of gas hydrate due to increased water temperature will occur after a lag time required for the thermal effect to penetrate deep into sediments. Our results shed light of the magnitude of the lag time; however, the range and duration of thermal fluctuations will be key factors determining the stability of shallow gas hydrate deposits. As the inventory of sites where such deposits occur continues to grow (e.g. [37]), one might expect that gas hydrate deposits in sites on the western margins (e.g. Gulf of Mexico) of ocean basins will be subject to a higher temperatures and greater thermal variability than those on eastern margins (e.g. Hydrate Ridge). This is because western boundary currents carry warm water from the tropics into higher latitudes and frequently spin off warm-cored eddies that impinge the slope, while eastern boundary currents are generally colder and slower [38]. The activity of the Gulf of Mexico Loop Current is probably responsible for the variable temperature regime of the Bush Hill site, although the dynamics of the process are as yet undetermined.

Shallow gas hydrate deposits are also potentially unstable because their density is less than seawater or marine sediment. We commonly observed chips of hydrate floating upward during our drilling operations, so it is clearly true that a piece of gas hydrate, freed from the sediment matrix, would rapidly exit the benthic environment. Many authors have similarly observed pieces of gas hydrate floating free from the bottom and surmised that this phenomenon could regularly produce cratering and pockmarks often associated with gas hydrate deposits [22,24] or, more exceptionally, cause large-scale excavation of gas hydrate and transfer to the upper water column [39]. The photographic time-series described in this paper comprised 350 days during which time the morphology of the mound was altered only in detail. This finding is consistent with a preliminary photographic time-series from Bush Hill [19]. The present findings provide no support for the theory that rafting of sediments and cratering of the seafloor by dislodged pieces of gas hydrate is a regular occurrence.

Present findings indicate that in-situ measurements of thermal diffusion in gas hydrate deposits, as well as surface sediments, are possible when the ambient temperatures are changing rapidly over a relatively broad range. The robust fit of these estimates to our field data suggests that geothermal heat flow due has not been perturbed by rapid gas or fluid flux. It would be interesting to implant thermistor probes into settings where rapid fluid or gas flux is expected and attempt to detected enhance heat flux as a result.

Estimates for the thermal diffusivity of this natural gas hydrate are lower than the diffusivity inferred from laboratory measurements of thermal conductivity, density and heat capacity would suggest. The considerable impurities found in the natural product (oil, sediment and organic matter) undoubtedly contribute to this difference, as laboratory experiments with mixtures of methane hydrate and quartz sand have suggested [33]. Autoregressive and finite element methods offer alternative approaches for modeling such data. Both work well in the simple two-thermistor case, but the finite element method would provide superior resolution if additional thermistors were added to the probes. Finding methods for drilling deeper into gas hydrate deposits and adding additional thermistors would improve the present methodology.

Spikes in bottom water temperatures have been attributed to be the cause of rapid increases in the flux of gas bubbles that have been measured escaping from gas hydrate deposits at Bush Hill [22,23]. The present results raise serious problems for this theory. The effect of relatively low thermal diffusion into gas hydrate is to dampen markedly the largest spikes in bottom water temperature. Addition of even a thin layer of sediment would additionally insulate buried deposits from any fluctuation above the annual mean. Although the hydrate deposit is an active biological substratum and is gradually increasing in size, on a yearly time scale, it appears to be a relatively stable component of the seep environment. Kinetic models of the Bush Hill hydrate deposit suggest that it has been accumulating for on the order of 10,000 yr [40]. While application of better thermal diffusion estimates might prove helpful for such efforts, our results support the long-term accumulation of gas hydrate at Bush Hill despite the variable temperature regime of the Gulf of Mexico slope.

Acknowledgements

We thank the personnel of the Harbor Branch Oceanographic Institution submersible operations for assistance at sea. Support from the U.S. Dept. of Energy National Energy Technology Laboratory, the National Science Foundation LExEN program (OCE-0085549), University of Mississippi (Subcontract No. 02-11-55) under US Department of Energy Contract No. DE-FC26-00NT40920 and the NOAA National Undersea Research Program, UNCW center is gratefully noted.

References

[1] K.A. Kvenvolden, Gas hydrates—geological perspective and global change, Rev. Geophys. 31 (2) (1993) 173–187.
[2] E.T. Peltzer, P.G. Brewer, Practical physical chemistry and empirical predictions of methane hydrate stability, in: M.D. Max (Ed.), Natural Gas Hydrate in Oceanic and Permafrost Environments, Coastal Systems and Continental Margins, Kluwer Academic Publishers, The Netherlands, 2000, pp. 17–28.
[3] G.J. MacDonald, Role of methane clathrates in past and future climates, Clim. Change 16 (1990) 247–281.
[4] G.R. Dickens, The potential volume of oceanic methane hydrates with variable external conditions, Org. Geochem. 32 (10) (2001) 1179–1193.
[5] R.D. Norris, U. Röhl, Carbon cycling and the chronology of climate warming during the Palaeocene/Eocene transition, Nature 401 (1999) 775–778.
[6] J.P. Kennett, K.G. Cannariato, Ingrid L. Hendy, Richard J. Behl, Carbon isotopic evidence for methane hydrate instability during quaternary interstadials, Science 288 (2000) 128–133.
[7] B.A. Buffett, O.Y. Zatsepina, Metastability of gas hydrate, Geophys. Res. Lett. 26 (19) (1999) 2981–2984.
[8] A.V. Milkov, R. Sassen, Thickness of the gas hydrate stability zone, Gulf of Mexico continental slope, Mar. Pet. Geol. 17 (9) (2000) 981–991.
[9] W.P. Dillon, M.D. Max, Oceanic gas hydrate, in: M.D. Max (Ed.), Natural Gas Hydrates in Oceanic and Permafrost Environments, Coastal Systems and Continental Margins, vol. 5, Kluwer Academic Press, The Netherlands, 2000, pp. 61–76.
[10] A.G. Yefremova, B.P. Zhizhchenko, Discovery of gas crystal hydrates in recent offshore sediments, Dokl. Akad. Nauk SSSR 214 (5) (1974) 1179–1181.
[11] G.D. Ginsburg, V.A. Soloviev, Submarine Gas Hydrates, VNIIOkeangeologia, St. Petersburg, Russia, 1998. 215 pp.
[12] J.M. Brooks, M.C. Kennicutt II, R.R. Fay, T.J. McDonald, R. Sassen, Thermogenic gas hydrates in the Gulf of Mexico, Science 223 (1984) 696–698.
[13] G. Ginsburg, R. Guseynov, A. Dadashev, G. Invanova, S. Kazantsev, V. Solov'yev, E. Telepnev, R. Askeri-Nasirov, A. Yesikov, Gas hydrates of the southern Caspian, Int. Geol. Rev. 34 (8) (1992) 765–782.
[14] G.D. Ginsburg, V.A. Soloviev, R.E. Cranston, T.D. Lorenson, K.A. Kvenvolden, Gas hydrates from the continental slope, offshore Sakhalin Island, Okhotsk Sea, Geo Mar. Lett. (13) (1993) 41–48.
[15] J.M. Brooks, M. Field, M.C. Kennicutt, Observations of gas hydrates in marine sediments, offshore northern California, Mar. Geol. 96 (1991) 103–109.
[16] G. Bohrmann, J. Greinert, E. Suess, M. Torres, Authigenic carbonates from the Cascadia subduction zone and their relation to gas hydrate stability, Geology 26 (7) (1998) 647–650.
[17] J.M. Brooks, W.R. Bryant, B.B. Bernard, N.R. Cameron, The nature of gas hydrates on the Nigerian continental slope, Gas Hydrates: Challenges for the Future, Annals of the New York Academy of Sciences, vol. 912, 2000, pp. 76–93.
[18] C.L. Van Dover, P. Aharon, J.M. Bernhard, E. Caylor, M. Doerries, W. Flickinger, W. Gilhooly, S.K. Goffredi, K.E. Knick, S.A. Macko, S. Rapoport, E.C. Raulfs, C. Ruppel, J.L. Salerno, R.D. Seitz, B.K. Sen Gupta, T. Shank, M. Turnipseed, R. Vrijenhoek, Blake Ridge methane seeps: characterization of a soft-sediment, chemosynthetically based ecosystem, Deep-Sea Res., Part 1 50 (2) (2003) 281–300.
[19] I.R. MacDonald, W.W. Sager, M.B. Peccini, Association of gas hydrate and chemosynthetic fauna in mounded bathymetry at mid-slope hydrocarbon seeps: northern Gulf of Mexico, Mar. Geol. 198 (2003) 133–158.

[20] I. Leifer, I.R. MacDonald, Dynamics of the gas flux from shallow gas hydrate deposits: interaction between oily hydrate bubbles and the oceanic environment, Earth Planet. Sci. Lett. 21 (3–4) (2003) 411–421.
[21] S.M. De Beukelaer, I.R. MacDonald, N.L. Guinnasso, J.A. Murray, Distinct side-scan sonar, RADARSAT SAR, and acoustic profiler signatures of gas and oil seeps on the Gulf of Mexico slope, Geo Mar. Lett. 23 (3–4) (2003) 177–186.
[22] I.R. MacDonald, N.L. Guinasso Jr., R. Sassen, J.M. Brooks, L. Lee, K.T. Scott, Gas hydrate that breaches the sea floor on the continental slope of the Gulf of Mexico, Geology 22 (1994) 699–702.
[23] H. Roberts, W. Wiseman Jr., J. Hooper, G. Humphrey, Surficial gas hydrates of the Louisiana continental slope—initial results of direct observations and in situ data collection, Offshore Technology Conference, vol. 10770, Offshore Technology Conference, Houston, TX, 1999, pp. 259–272.
[24] E. Suess, M.E. Torres, G. Bohrmann, R.W. Collier, J. Greinert, P. Linke, G. Rehder, A. Trehu, K. Wallmann, G. Winckler, E. Zuleger, Gas hydrate destabilization: enhanced dewatering, benthic material turnover and large methane plumes at the Cascadia convergent margin, Earth Planet. Sci. Lett. 170 (1–2) (1999) 1–15.
[25] I.R. MacDonald, R. Arvidson, R.S. Carney, C.F. Fisher, N.L. Guinasso Jr., S. Joye, P. Montagna, J.W. Morse, D.C. Nelson, E. Powell, W. Sager, R. Sassen, S. Schaeffer, G.A. Wolff, Stability and Change in Gulf of Mexico Chemosynthetic Communities: Final Report, U.S. Dept. Interior, Minerals Management Service, Gulf of Mexico OCS Region, Contract 14-35-001-31813, New Orleans, LA, 2002, p. 498.
[26] R. Sassen, I.R. MacDonald, N.L. Guinasso Jr., S. Joye, A.G. Requejo, S.T. Sweet, J. Alcala-Herrera, D.A. DeFritas, D.R. Schink, Bacterial methane oxidation in sea-floor gas hydrate: significance to life in extreme environments, Geology 26 (9) (1998) 851–854.
[27] E.D. Sloan, Clathrate Hydrates of Natural Gases, Marcel Drekker, Inc., New York, 1990, 641 pp.
[28] C.R. Fisher, I.R. MacDonald, R. Sassen, C.M. Young, S.A. Macko, S. Hourdez, R.S. Carney, S. Joye, E. McMullin, Methane ice worms: *Hesiocaeca methanicola* colonizing fossil fuel reserves, Naturwissenschaften 87 (4) (2000) 184–187.
[29] R. Nikolaus, J.W. Ammerman, I.R. MacDonald, Distinct pigmentation and trophic modes in Beggiatoa from hydrocarbon seeps in the Gulf of Mexico, Aquat. Microb. Ecol. 32 (2003) 85–93.
[30] H.S. Carslaw, J.C. Jaeger, Conduction of Heat in Solids, Clarendon Press, Oxford, UK, 1959, 510 pp.
[31] D. Davidson, Gas hydrates as clathrate ices, in: J. Cox (Ed.), Natural Gas Hydrates—Properties, Occurrence and Recovery, Butterworth, Woburn, MA, 1983, pp. 1–16.
[32] S.E. Prensky, A review of gas hydrates and formation evaluation of hydrate-bearing reservoirs, Society of Professional Well Log Analysts, 1995, p. GGG, Paris, France.
[33] W.F. Waite, B.J. deMartin, S.H. Kirby, J. Pinkston, C.D. Ruppel, Thermal conductivity measurements in porous mixtures of methane hydrate and quartz sand, Geophys. Res. Lett. 29 (24) (2002).
[34] R.D. Stoll, B. G.M., Physical properties of sediments containing gas hydrates, J. Geophys. Res., [Solid Earth] 84 (B4) (1979) 1629–1634.
[35] R. von Herzen, A.E. Maxwell, The measurement of thermal conductivity of deep-sea sediments by a needle-probe method, J. Geophys. Res. 64 (1959) 1557–1663.
[36] M. Hutnak, M.E. Torres, H.P. Johnson, R.W. Collier, Periodic negative heat flow on southern hydrate ridge: implications for the destabilization of gas hydrates, Eos 80 (46) (1999) F482.
[37] K.A. Kvenvolden, Gas hydrate and humans, Gas Hydrates: Challenges for the Future, Annals of the New York Academy of Sciences, vol. 912, 2000, pp. 17–22.
[38] G.L. Pickard, W.J. Emery, Descriptive Physical Oceanography, 5th edition, Butterworth and Heinemann, Boston MA, 2002, 320 pp.
[39] C.K. Paull, P.G. Brewer, W. Ussler, E.T. Peltzer, G. Rehder, D. Clague, An experiment demonstrating that marine slumping is a mechanism to transfer methane from seafloor gas-hydrate deposits into the upper ocean and atmosphere, Geo Mar. Lett. 22 (4) (2003) 198–203.
[40] D.F. Chen, L.M. Cathles, A kinetic model for the pattern and amounts of hydrate precipitated from a gas steam: application to the Bush Hill vent site, Green Canyon Block 185, Gulf of Mexico, J. Geophys. Res. [Solid Earth] 108 (B1) (2003).